Open Forum Infectious Diseases

MAJOR ARTICLE

Manganese Breaks the Immune Tolerance of HBs-Ag

Mengxin Lin,[1,a] Ruyi Guo,[1,a] Cuiping Ma,[1] Dawu Zeng,[2] and Zhijun Su[1]

[1]Department of Infectious Disease, Quanzhou First Hospital Affiliated to Fujian Medical University, Quanzhou, Fujian, China, and [2]Liver Research Center, the First Affiliated Hospital of Fujian Medical University, Taijiang District, Fuzhou, Fujian, China

Background. Manganese (Mn^{2+}) has been shown to promote type I interferon (IFN) production and activate the cyclic GMP-AMP synthase (cGAS)/Stimulator of Interferon Genes (STING) signaling pathway, suggesting that Mn^{2+} could be used as an adjuvant for vaccination.

Methods. In present study, the effects of Mn^{2+} on vaccination against hepatitis B virus (HBV) were evaluated. We treated mouse hepatocytes and kuppfer cells with Mn^{2+} with or without adeno-associated virus (AAV)–HBV infection. Expression of IFN-α and IFN-β and activation of TBK1 and IRF3 were monitored. Wild-type and $STING^{-/-}$ mice were treated with Mn^{2+} and then infected with AAV-HBV. Serum levels of HBV surface antigen (HBsAg), alanine aminotransferase (ALT) activity, IFN-α, and IFN-β were detected. Lymphocyte infiltration in the liver was evaluated. HBsAg-Tg mice were vaccinated with Mn^{2+} and HBsAg. The serum levels of HBsAg antibody, alanine transaminase activity, and IFN-β were monitored after vaccination.

Results. Mn^{2+} promoted IFN-α and IFN-β production in mouse hepatocytes and kuppfer cells. Mn^{2+} failed to promote IFN-α and IFN-β production in kuppfer cells deficient in STING. Mn^{2+} promoted activation/phosphorylation of TBK1 and IRF3 during AAV-HBV infection. Mn^{2+} decreased serum levels of HBsAG, increased serum levels of alanine aminotransferase (ALT), IFN-α and IFN-β, and enhanced lymphocyte infiltration and the percentage of IFN-γ-producing $CD8^+$ T cells in the liver of AAV-HBV-infected mice. In contrast, Mn^{2+} treatment did not affect serum levels of HBsAG, ALT, IFN-α, or IFN-β in STING-deficient mice.

Conclusions. Mn^{2+} promoted HBsAG antibody, ALT, and IFN-β production after HBsAG immunization. Mn^{2+} promoted type I IFN production in AAV-HBV infection and HBsAG immunization and could be used as an adjuvant for vaccination.

Keywords. HBV; manganese; type I IFN; vaccine.

Human hepatitis B virus (HBV) infection affects more than one-third of the world's population [1]. Despite the implementation of the HBV vaccine, there are ~40 million chronic HBV infections and 100 million people positive for HBV surface antigen (HBsAg) in the world. These people are at high risk of developing liver carcinoma [2].

Antiviral therapy has been utilized to prevent advanced liver disease development and decrease HBV infection–caused mortality, a crucial goal of which is loss of HBsAg [3]. Interferon (IFN)-based antiviral therapies have been used for HBV infection treatment [4, 5]. IFNs are a group of signaling proteins produced and secreted when host cells encounter pathogen infection [6, 7]. Human IFNs are classified into type I, II, and III according to the receptor they bind to [8]. IFN-α and IFN-β belong to type I IFN and have been approved to treat HBV [9]. In addition, both IFN-α and IFN-β have been described to inhibit HBV replication in in vitro systems [10, 11]. Therefore, enhancing IFN production could be a criterion of therapeutic treatment for HBV.

A recent publication described that manganese (Mn) is essential in host defense against DNA viruses [12]. Upon DNA virus infection, Mn^{2+} is released and accumulated in the host cell cytosol. Mn^{2+} directly binds to cyclic GMP-AMP synthase (cGAS) and activates the cGAS/Stimulator of Interferon Genes (STING) signaling pathway, which results in production of type I IFN. In contrast, Mn-deficient mice have decreased cytokine production and are more susceptible to DNA virus infection. These results suggest that Mn^{2+} could be utilized as an adjuvant to boost immune response in vaccination. In present study, we investigated the effects of Mn^{2+} on boosting immune response using the adeno-associated virus (AAV)–HBV model.

METHODS

Reagents

Anti-TBK1 was obtained from Santa Cruz Biotechnology (Dallas, TX, USA). Anti-β actin was obtained from Sigma (St. Louis, MO, USA). Anti-Phospho-TBK1 (pTBK1, Ser172), anti-phospho-IRF-3 (Ser396), and anti-IRF-3 were purchased from Cell Signaling Technology (Danvers, MA, USA).

Received 29 July 2020; editorial decision 15 January 2021; accepted 21 January 2021.

[a]Equal contribution

Correspondence: Zhijun Su, Department of Infectious Disease, Quanzhou First Hospital Affiliated to Fujian Medical University, No. 250 East Street, Quanzhou 362000, Fujian, China (sudoc2366@126.com).

Open Forum Infectious Diseases®2021

DOI: 10.1093/ofid/ofab028

Anti-HBsAg was purchased from Abcam (Shanghai, China). For flow cytometry, PE-conjugated anti-IFN-γ and APC-CY7-conjugated anti-CD8 were purchased from eBioscience (San Diego, CA, USA). Manganese (II) chloride tetrahydrate $MnCl_2 \cdot 4H_2O$ and manganese (II) acetate dehydrate $Mn(OAc)_2 \cdot 2H_2O$ were obtained from Sigma-Aldrich (St. Louis, MO, USA). The HBsAg was purified from CHO cells expressing recombinant HBsAg vaccine (rHBVvac; China North Pharmaceutical Group Corporation, Shijiazhuang, China) as described previously [13].

Mice Treatment

Eight-week-old C57BL/6 mice, 8-week-old $Tlr9^{em1.1Ldm}$/J mice, and $Sting1^{gt}$/J on C57BL/6 background were purchased from the Animal Model Research Center of Nanjing University. HBsAg transgenic mice (C57BL/6J-Tg(A1b1HBV)44Bri/J mice) were purchased from the Animal Center of the Shanghai Public Health Clinical Center (Shanghai, China).

Mice were pretreated with 1 mg/kg of $MnCl_2$ for 24 hours and then infected with AAV/HBV at 5×10^{10} viral genome equivalents through tail vein injection. Animal studies were reviewed and approved by the ethics commitment of Quanzhou First Hospital Affiliated to Fujian Medical University.

AAV-HBV Infection

AAV/HBV virus (AAV8) was provided by Beijing FivePlus Molecular Medicine Institute (Beijing, China). The recombinant virus with indicated amount was diluted to 200 μL of phosphate-buffered saline (PBS) and then injected into C57BL/6 mice through tail vein injection. After infection, blood was collected by retrobulbar bleeding for analysis.

Primary Mouse Hepatocyte and Kupffer Cell Isolation and Treatment

Livers were harvested from 8-week-old mice. Hepatocytes were isolated using a modified 2-step collagenase perfusion protocol as described previously [14]. The hepatocytes were cultured in DMEM/F12-containing supplements using collagen I-coated dishes as described previously [15]. Mouse kupffer cells were isolated following a protocol described previously [16]. Cells were treated with different concentrations of $MnCl_2$ or $Mn(OAc)_2$. In an experiment, cells were pretreated with 100 μM of $MnCl_2$ or $Mn(OAc)_2$ for 24 hours and then stimulated with AAV-HBV (10 MOI). Samples were collected at indicated time points.

Histology

Seven days post–AAV-HBV infection, livers were harvested, fixed, and paraffin-embedded. Four-micrometer sections were obtained for hematoxylin and eosin (H&E) staining and histopathological evaluation.

Enzyme-Linked Immunosorbent Assay

Serum alanine aminotransferase activity was determined using an alanine aminotransferase (ALT) kit (BioSino Bio-technology and Science Inc, Beijing, China). Serum levels of HBV antibodies were monitored using a commercial enzyme-linked immunosorbent assay (ELISA) kit (BioSino Bio-technology and Science Inc, Beijing, China).

RT-PCR

Total RNA from mouse hepatocytes and Kuffer cells was extracted using the NucleoSpin RNA Plus kit (Takara, Beijing, China). The PrimeScript RT Reagent Kit (Takara, China) was used for cDNA synthesis. Real-time quantitative PCR reactions were set up in triplicate using TB Green Advantage qPCR Premix (Takara, China) and performed using the QuantStudio 3 Real-time PCR System (Applied Biosystems, Waltham, MA, USA). Sequences of primers for real-time PCR were *IFN-α* sense 5'- AGTCCATCAGCAGCTCAATGAC -3'; antisense 5'- AAGTATTTCCTCACAGCCAGCAG -3'; *IFN-β* sense 5'- AGCTCCAAGAAAG GACGAACAT -3'; antisense 5'- GCCCTGTAGGTGAGGTTGATCT -3'; *Isg15* sense 5'- CTA GAGCTAGAGCCTGCAG -3'; antisense 5'-AGTTAGTCACGGACACCAG -3'. *Oasl1* sense 5'- TGAGCG CCCCCCATCT -3'; *Oasl1* antisense CATGACCCAGGACAT CAAAGG; *β-actin* sense 5'-GAAATCGT GCGTGACATCAA AG-3'; antisense 5'-TGTAGTTTCATGGATG CCACAG-3'.

Statistical Analysis

Statistical difference was determined using the Student *t* test or 1-way analysis of variance with Tukey's post hoc test using Prism software. Statistical differences were considered significant at a P value <.05.

RESULTS

Mn^{2+}-Induced Type I IFN Production in Mouse Hepatocytes

It has been described that Mn^{2+} induces type I IFN production [12]. To investigate the effects of Mn^{2+} on type I IFN production in mouse primary hepatocytes, mouse primary hepatocytes were treated with different concentrations of $MnCl_2$ or $Mn(OAc)_2$ for 12 hours. Then mRNA and protein levels of IFN-α and IFN-β were measured. As shown in Figure 1A, both $MnCl_2$ and $Mn(OAc)_2$ treatment for 12 hours induced IFN-α and IFN-β mRNA expression in mouse primary hepatocytes in a dose-dependent manner. At the same concentration, $MnCl_2$ treatment induced higher mRNA levels of IFN-α and IFN-β than $Mn(OAc)_2$ treatment. Correspondingly, Mn^{2+} treatment induced IFN-α and IFN-β protein production in a dose-dependent manner (Figure 1B). We further investigated these effects in the presence of infection. We pretreated mouse hepatocytes with 100 μM of $MnCl_2$ for 1 hour and then stimulated the hepatocytes with 10 MOI AAV-HBV. As shown in Figure 1C, in cells only stimulated with AAV-HBV, AAV-HBV stimulation

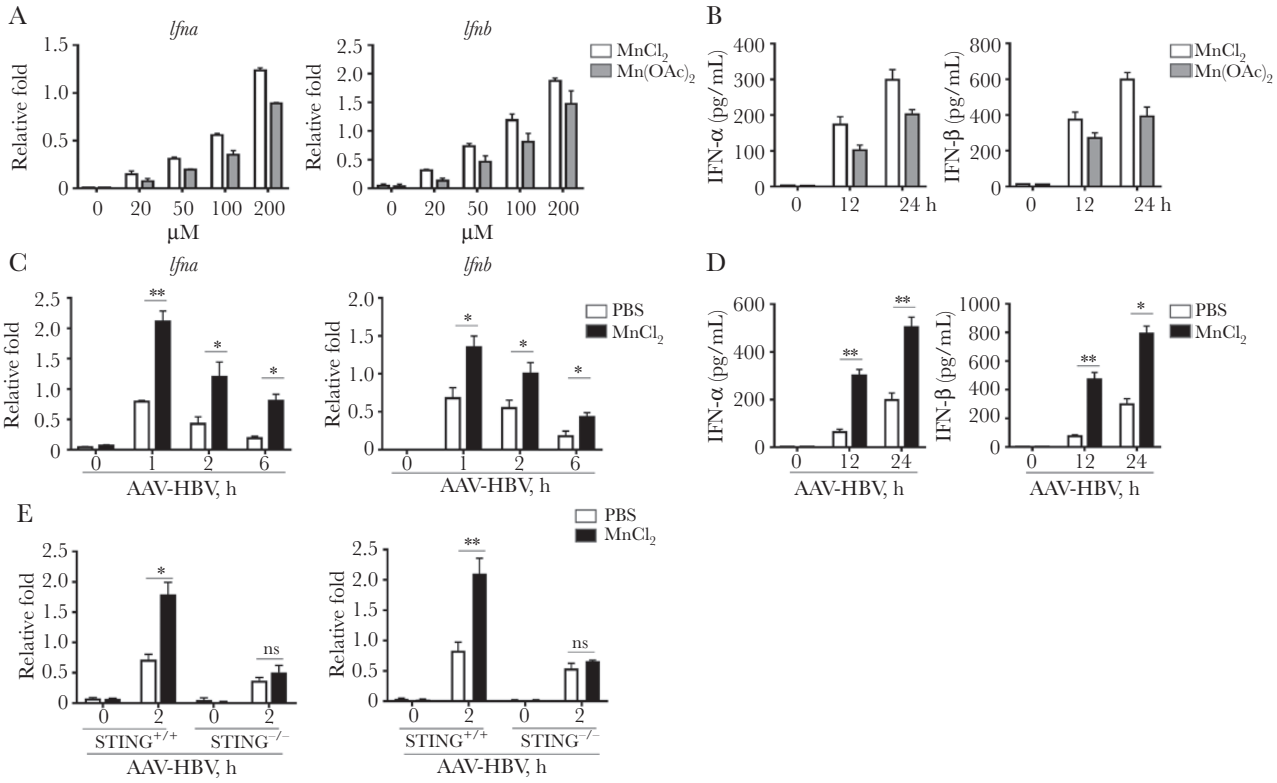

Figure 1. Mn^{2+} induces the production of type I IFN in mouse hepatocytes. A and B, Mouse primary hepatocytes were stimulated with different doses of Mn^{2+} for 12 hours. At different time points, the expression of type I interferons was measured by qRT-PCR (A) and ELISA assay (B). C and D, Mouse primary hepatocytes were pretreated with 100 μM of Mn^{2+} for 24 hours and then stimulated with AAV-HBV (10 MOI). At indicated time points, the expression of type I interferons was measured by qRT-PCR (C) and ELISA assay (D). E, Primary mouse hepatocytes from WT or $STING^{-/-}$ mice were pretreated with 100 μM of Mn^{2+} for 1 hour and stimulated with AAV-HBV (10 MOI) at indicated time points. The expression of type I interferons was measured by qRT-PCR. All data are presented as fold relative to the β actin mRNA level. Data are presented as mean ± SEM values and are representative of at least 3 independent experiments. Statistical analyses represent variations in experimental replicates. $^{*}P < .05$; $^{**}P < .01$. Abbreviations: AAV-HBV, adeno-associated human hepatitis B; ELISA, enzyme-linked immunosorbent assay; IFN, interferon; PBS, phosphate-buffered saline; qRT-PCR, quantitative reverse transcription polymerase chain reaction; SEM, standard error of mean; STING, stimulator of interferon genes; WT, wild type.

induced IFN-α and IFN-β mRNA expression, which reached the peak at 1 hour post–AAV-HBV stimulation and decreased as time increased. In contrast, cells pretreated with $MnCl_2$ and then stimulated with AAV-HBV had significantly higher mRNA levels at each time point when compared with cells only stimulated with AAV-HBV, indicating that Mn^{2+} promoted AAV-HBV-induced type I IFN production. Correspondingly, we detected significantly increased IFN-α and IFN-β released from Mn^{2+}-pretreated AAV-HBV-stimulated cells, when compared with AAV-HBV-stimulated cells (Figure 1D). Furthermore, Mn^{2+} did not promote the AAV-HBV-induced production of IFN-α and IFN-β in hepatocytes from $STING^{-/-}$ mice (Figure 1E), indicating the Mn^{2+}-induced IFN-α and IFN-β production depended on STING. Collectively, these results demonstrated that Mn2+ promoted type I IFN production in mouse hepatocytes.

Mn^{2+} Promoted Type I IFN Expression in Mouse Kupffer Cells

We continued to investigate whether Mn^{2+} promoted type I IFN expression in Kupffer cells. Consistent with the results from hepatocytes, we detected significantly increased IFN-α mRNA in $MnCl_2$-treated/AAV-HBV-stimulated Kupffer cells at 2 hours and 6 hours post–AAV-HBV stimulation when compared with AAV-HBV-stimulated hupper cells. Similarly, the IFN-β mRNA in $MnCl_2$-treated/AAV-HBV-stimulated huppffer cells was significantly higher than that in AAV-HBV-stimulated huppffer cells at 1 hour, 2 hours, and 6 hours post–AAV-HBV stimulation (Figure 2A). Correspondingly, $MnCl_2$ treatment significantly increased mRNA levels of Isg15 and oasl, 2 IFN-induced genes, at 6 hours post–AAV-HBV stimulation (Figure 2B). Furthermore, decreased viral load partially impaired the inductions of the proinflammatory cytokines (Figure 2C). These results demonstrated that Mn^{2+} promoted type I IFN expression in mouse Kupffer cells. As Mn^{2+}-induced type I IFN production has been shown to depend on the cGAS-STING pathway [12], we continued to investigate whether this would also be the case in our study. We pretreated Kupffer cells from TLR9-deficient mice and STING-deficient mice with Mn^{2+} and stimulated cells with AAV-HBV. As shown in Figure 2D, AAV-HBV stimulation resulted in increased mRNA levels of IFN-α and IFN-β in Kupffer cells from

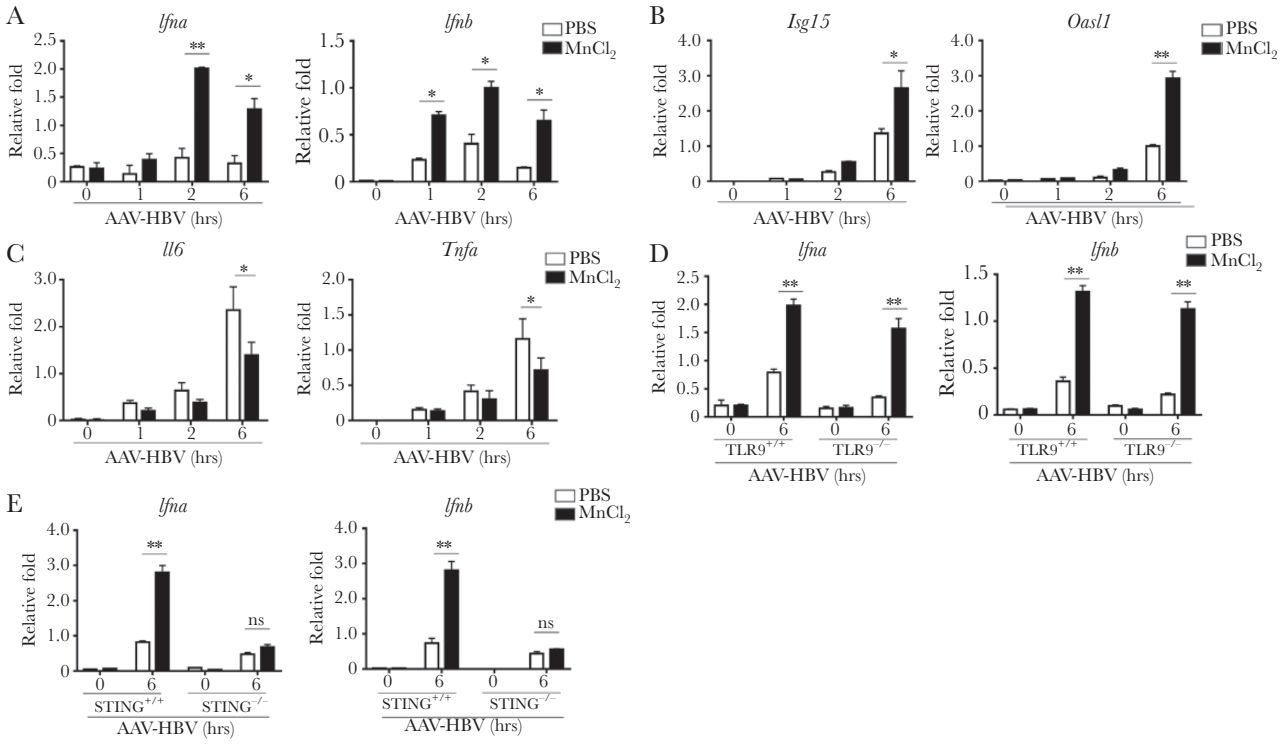

Figure 2. Mn^{2+} also significantly upregulates the expression of type I IFN in mouse Kupffer cells. A and B, Mouse primary Kupffer cells were pretreated with 100 μM of Mn^{2+} for 1 hour and then stimulated with AAV-HBV (10 MOI) at indicated time points. The expression of type I interferons was measured by qRT-PCR (A) and ELISA assay (B). C, The induction of *Il6* and *Tnfa* was measured in Kupper cells treated with $MnCl_2$ by qRT-PCR. D and E, Primary Kupffer cells from WT or $STING^{-/-}$ mice were pretreated with 100 μM of Mn^{2+} for 1 hour and stimulated with AAV-HBV (10 MOI) at indicated time points. Expression of type I interferons was measured by qRT-PCR (D) and ELISA assay (E). All data are presented as fold relative to the Actb mRNA level. Data are presented as mean ± SEM values and representative of at least 3 independent experiments. Statistical analyses represent variations in experimental replicates. $^{*}P < .05$; $^{**}P < .01$. Abbreviations: AAV-HBV, adeno-associated human hepatitis B; ELISA, enzyme-linked immunosorbent assay; IFN, interferon; Il6, interleukin 6; Isg15, IFN-stimulated genes 15; PBS, phosphate-buffered saline; qRT-PCR, quantitative reverse transcription polymerase chain reaction; SEM, standard error of mean; STING, stimulator of interferon genes; Tnfa, tumor necrosis factor a; WT, wild type.

wild-type mice, and Mn^{2+} treatment promoted mRNA expression of IFN-α and IFN-β after AAV-HBV stimulation. AAV-HBV stimulation failed to induce robust IFN-α and IFN-β expression in Kupffer cells from TLR9-deficient mice. In contrast, Mn^{2+} treatment still promoted mRNA expression of IFN-α and IFN-β in Kupffer cells from TLR9-deficient mice (Figure 2D). AAV-HBV stimulation induced mRNA expression of IFN-α and IFN-β in Kupffer cells from wild-type mice and $STING^{-/-}$ mice (Figure 2E). However, Mn^{2+} only promoted IFN-α and IFN-β expression in Kupffer cells from wild-type but not $STING^{-/-}$ mice. Collectively, our data suggest that AAV-HBV-induced expression of IFN-α and IFN-β depended on TLR9 and that Mn^{2+}-induced expression of IFN-α and IFN-β depended on STING.

Mn^{2+}-Activated TBK1-IRF3 Signal Pathway

As Mn^{2+} induced IFN-α and IFN-β expression through STING, we continued to investigate the effects of Mn^{2+} on activation of STING downstream pathways. We found that the high dose of Mn2+ induced more expressions of type I interferons, suggesting that the effect of Mn^{2+} was dose dependent (Figure 3A). As shown in Figure 3B, pretreatment of either $Mn(OAc)_2$ or $MnCl_2$ decreased the expression of HBcAg antigen after AAV-HBV infection in a dose-dependent manner, indicating that Mn^{2+} promoted the antiviral response and clearance of AAV-HBV. $MnCl_2$ pretreatment resulted in increased protein levels of phosphorylated-TBK1 and phosphorylated-IRF3 in a dose-dependent manner (Figure 3C), indicating that Mn^{2+} activated TBK1 and IRF3. In addition, AAV-HBV stimulation activated TBK1 and IRF3, and we detected the most abundant phospho-TBK1 and phosphor-IRF3 levels at 30 minutes poststimulation (Figure 3D). Consistently, $MnCl_2$ pretreatment promoted higher protein levels of phospho-TBK1 and phosphor-IRF3 at each time point post–AAV-HBV stimulation when compared with PBS pretreatment, further confirming that Mn^{2+} promotes the activation of the TBK1-IRF3 signal pathway.

Mn^{2+} Promoted Antiviral Immune Response in Mice

Next, we evaluated the effects of Mn^{2+} in vivo. We pretreated mice with Mn^{2+} followed by AAV-HBV infection. Fourteen days postinfection, a significantly decreased serum level of antigen HBsAg was detected in Mn^{2+}-treated mice when compared with PBS-treated mice (Figure 4A). Significant elevations in ALT levels (Figure 4B) and IFN-α and IFN-β (Figure 4C) were observed in serum samples from in Mn^{2+}-treated mice. We evaluated liver tissue sections and found more lymphocyte

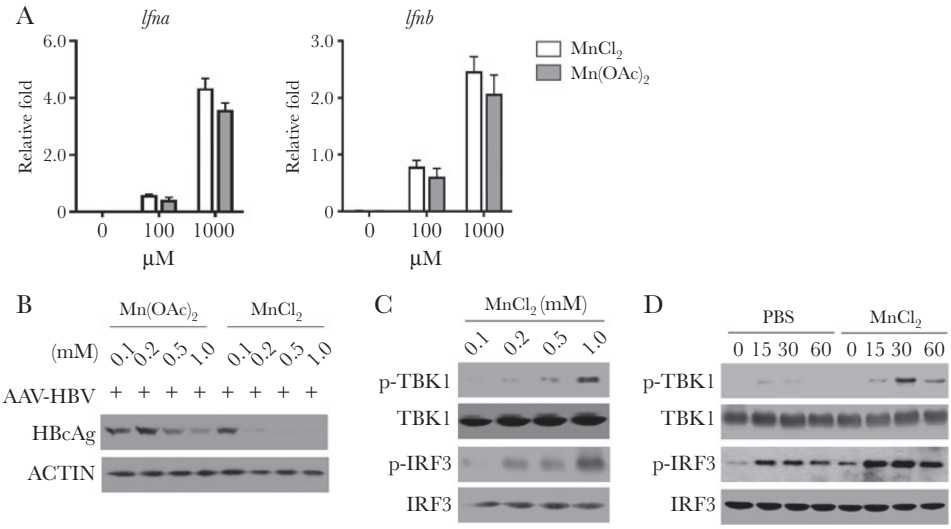

Figure 3. Mn^{2+} promotes the activation of the TBK1-IRF3 signal pathway. A, Mouse primary hepatocytes were stimulated with 1000 μM or 1 mM of Mn^{2+} for 12 hours. Expression of type I interferons was measured by qRT-PCR. B and C, Mouse primary hepatocytes were treated with different concentrations of $MnCl_2$ or $Mn(OAc)_2$, together with AAV-HBV (10 MOI), for 24 hours. Viral expression (B) and activation of TBK1-IRF3 (C) were determined by Western blot. D, Mouse primary hepatocytes were treated with 100 μM of $MnCl_2$ and infected AAV-HBV (10 MOI). Activation of TBK1-IRF3 was monitored at indicated time points after treatment. Data are representative of at least 3 independent experiments. Statistical analyses represent variations in experimental replicates. Abbreviations: AAV-HBV, adeno-associated human hepatitis B; IFN, interferon; IRF3, interferon regulatory factor 3; PBS, phosphate-buffered saline; qRT-PCR, quantitative reverse transcription polymerase chain reaction; TBK1, TANK-binding kinase 1.

infiltration in the liver from Mn^{2+}-treated mice (Figure 4D). Correspondingly, after stimulation with rHBsAg, there were significantly increased IFN-γ-producing $CD8^+$ T cells in the $CD8^+$ T-cell population purified from liver of Mn^{2+}-treated mice, when compared with liver from PBS-treated mice (Figure 4E). Collectively, these data show that Mn^{2+} promoted antiviral immune response after AAV-HBV infection.

Mn^{2+} Functioned as an rHBV Vaccine Adjuvant and Broke the Immune Tolerance in HBsAg-Tg Mice

Next, we investigated whether the effects of Mn^{2+} in vivo also required STING. Wild-type and $STING^{-/-}$ mice were pretreated with $MnCl_2$ and then infected with AAV/HBV. Significantly decreased serum levels of HBsAg were observed in wild-type mice treated with $MnCl_2$ when compared with wild-type mice treated with PBS

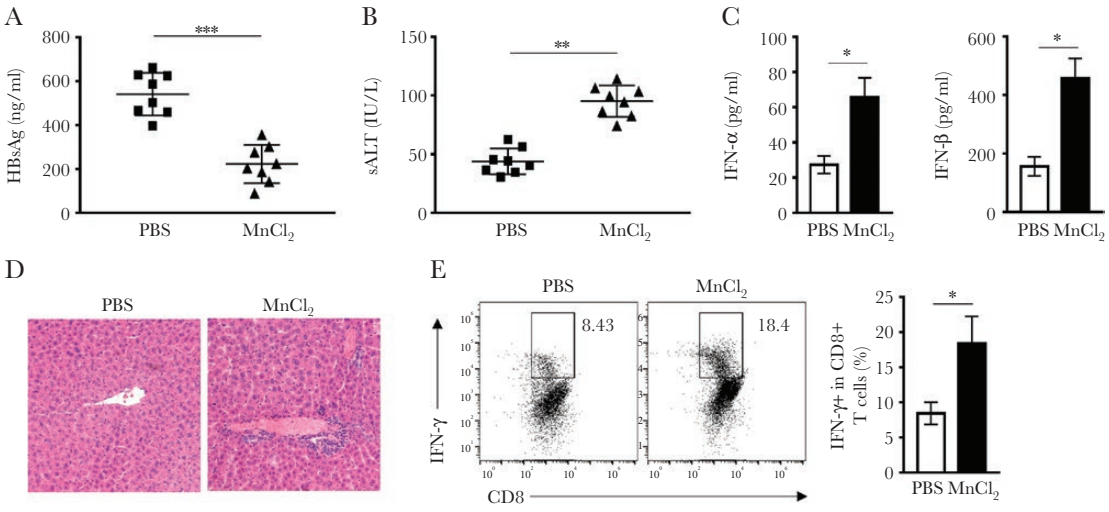

Figure 4. Mn^{2+} promoted AAV-HBV-induced antiviral immunity. A, C57BL/6 mice were pretreated with 1 mg/kg of $MnCl_2$ for 24 hours and then infected with AAV/HBV at 5×10^{10} viral genome equivalents through tail vein injection. At 14 days postinfection, blood samples were collected and serum HBsAg was measured by ELISA. ALT levels (B) and type I interferon expression (C) in serum of AAV-HBV-infected mice were measured by ELISA at day 14. D, H&E staining of liver sections from mice infected with AAV-HBV described as above. E, Intracellular staining of IFN-γ in $CD8^+$ T cells from liver stimulated with rHBsAg (10 μg/mL) for 3 days. Data are presented as mean ± SEM values and are representative of at least 3 independent experiments. Statistical analyses represent variations in experimental replicates. $^*P < .05$; $^{**}P < .01$; $^{***}P < .005$. Abbreviations: AAV-HBV, adeno-associated human hepatitis B; ALT, alanine aminotransferase; ELISA, enzyme-linked immunosorbent assay; HBsAg, HBV surface antigen; H&E, hematoxylin and eosin; IFN, interferon; PBS, phosphate-buffered saline; SEM, standard error of mean.

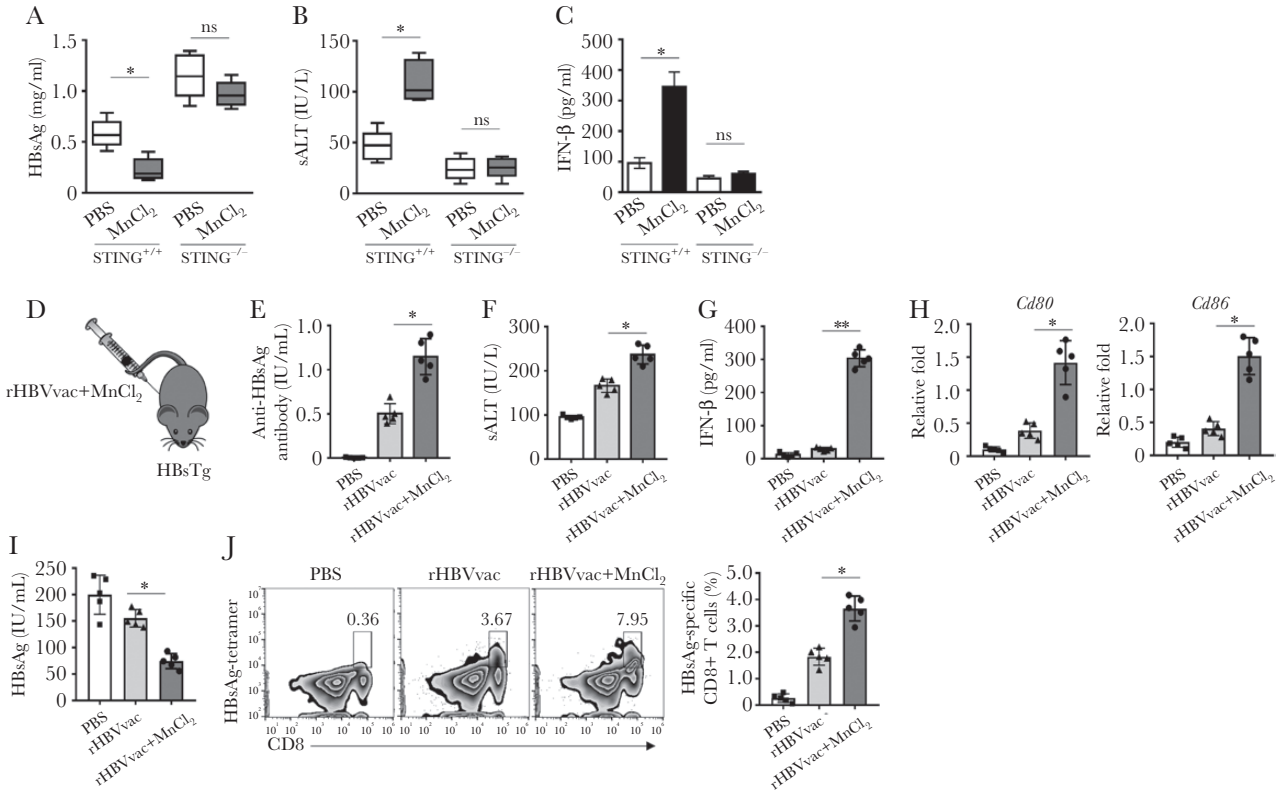

Figure 5. Mn^{2+} functions as vaccine adjuvant and breaks the immune tolerance of HBsAg-Tg mice. A, WT or STING$^{-/-}$ mice were pretreated with 1 mg/kg of $MnCl_2$ for 24 hours and then infected with AAV/HBV at 5×10^{10} viral genome equivalents through tail vein injection. At 14 days postinfection, blood samples were collected and serum HBsAg was measured by ELISA. ALT levels (B) and type I interferon expression (C) in serum of AAV-HBV-infected mice were measured by ELISA at day 14. D, Schematic illustration of the immunization regimen. HBsAg-Tg mice were immunized with $MnCl_2$ (1 mg/kg) and rHBV (1 μg) as shown. Mice were immunized on days 0, 14, and 28. E and F, Total serum anti-HBsAg IgG (E) and ALT levels (F) were analyzed on the seventh day after the third immunization. G, Type I interferon expression and HBsAg in serum of HBsAg-Tg-immunized mice were measured by ELISA. H, The CD11C+ DCs in draining lymph nodes were isolated by FACS. The mRNA levels of Cd80 and Cd86 in these DCs were measured by qPCR. I, The level of HBsAg in serum of HBsAg-Tg-immunized mice was measured by ELISA. J, Representative flow cytometric graphs showing HBsAg-specific CD8+ T cells in the liver of HBsAg-tg mice treated as indicated. Data are presented as mean ± SEM values and are representative of at least 3 independent experiments. Statistical analyses represent variations in experimental replicates. $^{*}P < .05$; $^{**}P < .01$. Abbreviations: AAV-HBV, adeno-associated human hepatitis B; ALT, alanine aminotransferase; DCs, dendritic cells; ELISA, enzyme-linked immunosorbent assay; HBsAg, HBV surface antigen; HBV, human hepatitis B; H&E, hematoxylin and eosin; IFN, interferon; PBS, phosphate-buffered saline; qPCR, quantitative polymerase chain reaction; SEM, standard error of mean; WT, wild type.

(Figure 5A). In contrast, there was no difference of in serum HBsAg levels between PBS-treated and $MnCl_2$-treated STING$^{-/-}$ mice. Interestingly, the serum levels of HBSAg in STING$^{-/-}$ mice were much higher than in wild-type mice, indicating that the STING$^{-/-}$ mice were more vulnerable to viral infection. The serum levels of ALT in $MnCl_2$-treated wild-type mice were significantly higher than in PBS-treated wild-type mice, while there was no difference in serum ALT levels between PBS-treated and $MnCl_2$-treated STING-deficient mice (Figure 5B). $MnCl_2$ treatment only promoted IFN-β expression in wild-type mice but not in STING$^{-/-}$ mice (Figure 5C). These results suggest that Mn^{2+} also functioned in vivo and that the function depended on STING. As Mn^{2+} promoted the immune response, we further evaluated its role as an adjuvant in vaccination. We immunized HBsAg-Tg mice with recombinant HBsAg antigen (rHBVvac) with or without $MnCl_2$, as presented in Figure 5D. Mice immunized with rHBVvac had enhanced serum levels of anti-HBsAg antibody. Immunization of rHBVvac and $MnCl_2$ resulted in higher anti-HBsAg antibody levels when compared with immunization of rHBV alone (Figure 5E). Immunization with rHBVvac resulted in increased serum levels of ALT (Figure 5F) and IFN-β (Figure 5G) when compared with immunization with PBS. Immunization of rHBV and $MnCl_2$ promoted serum levels of ALT (Figure 5F) and IFN-β (Figure 5G), when compared with immunization of rHBV alone. Our data demonstrate that rHBV and $MnCl_2$ clearly enhanced the mRNA levels of *Cd80* and *Cd86* (Figure 5H) and reduced the level of serum HBsAg (Figure 5I). Interestingly, a higher proportion of HBsAg-specific CD8+ T cells appeared in the liver of HBs-tg mice treated with rHBVvac and $MnCl_2$, compared with the rHBVvac control group (Figure 5J). Collectively, these results indicate that Mn^{2+} broke the immune tolerance and promoted immune response in HBsAg-Tg mice.

DISCUSSION

Mn is critical for many physiological processes including innate immunity. Here we evaluated the effects of manganese as a vaccine adjuvant using an AAV-HBV infection model. We

demonstrated Mn^{2+}-promoted type I IFN production in AAV-HBV-infected mouse hepatocytes and Kupffer cells, which depended on STING but not TLR9. Mn^{2+} promoted the activation of TBK1/IRF3 signaling. In addition, Mn^{2+} promoted IFN production and lymphocyte recruitment in mice and cleared AAV-HBV infection more efficiently. These effects were abolished in STING-deficient mice. Finally, we demonstrated that Mn^{2+} promoted antibody and IFN production after HBsAg immunization. These results suggest that Mn^{2+} could be used as an adjuvant for vaccination.

Mn is an essential component and necessary cofactor of several enzymes and proteins including photosynthesis system II and superoxide dismutase [17]. Mn has been described to be associated with disease [18]. The role of Mn in innate immunity has been described too. Wang et al. described that human macrophage–like cell THP-1 supplemented with medium containing Mn^{2+} and mice supplemented with diet containing Mn^{2+} are more resistant to viral infection, which was due to the augmented production of type I IFN [12]. In their study, they treated THP-1 cells directly treated with Mn^{2+} and observed significantly increased type I IFN production. In current study, we treated mouse hepatocytes with Mn^{2+} and observed increased type I IFN production, indicating that induction of type I IFN by Mn^{2+} could be a common feature that is independent of cell types.

The underlying mechanisms of how Mn^{2+} induced type I IFN have also been elucidated. We found that Mn^{2+} treatment activated the phosphorylation of TBK1 and IRF3. In addition, Mn^{2+}-induced type I IFN production was abolished in Kupffer cells from STING-deficient mice. These results suggest that Mn^{2+} induced IFN production through the STING signaling pathway. Our findings were consistent with the previous report. Wang et al. found that deficiency of cGAS, STING, TBK1, or IRF3 abrogated Mn^{2+}-induced type I IFN production [12]. The cGAS-STING pathway detects the cytosolic DNA and activates downstream signals. Upon binding DNA, cGAS converts GTP and ATP to cyclic GMP-AMP (cGAMP). cGAMP then binds to STING and phosphorylates TBK1 and IRF3. IRF3 is translocated into the cell nucleus and triggers transcription of inflammatory genes including IFN-α and INF-β.

IFN-α and INF-β are type I IFN. Upon binding to the IFN-a/β receptor, IFN-α and INF-β activate the intracellular Jak/Stat signaling pathway and activate the transcription of IFN-stimulated genes (ISGs). Many ISGs have been shown to inhibit HBV replication. For example, Lucifora and colleagues reported that IFN-α induced the expression of APOBEC3A/B, which resulted in cytidine deamination and degradation of covalently closed circular DNA (cccDNA), which prevented HBV reactivation [19]. MxA was an IFN-inducible cytoplasmic dynamin-like GTPase that interacted with hepatitis B core antigen (HBcAg) and interfered with the formation of HBV core particle [20].

The manganese salt has been suggested as a potent universal adjuvant by Zhang et al. [21]. Their study demonstrated that intranasal administration of colloidal manganese salt promoted dendritic cell maturation and antigen-specific T-cell activation and induced high levels of IgA antibodies. Therefore, Mn^{2+} itself was an effective stimulator of innate immune response and induced production of type I IFN and cytokines in the absence of infection. In the presence of viral infection, Mn^{2+} sensitized both cGAS and STING. Mn^{2+} increased both the DNA sensitivity and enzyme activity of cGAS. Mn^{2+} enhanced cGAMP-STING binding affinity, resulting in increased STING activity [12]. In the present study, we also demonstrated that Mn^{2+} promoted type I IFN production in the presence of AAV-HBV infection, suggesting that a common feature of Mn^{2+} may be the promotion of innate immune response against viral infection. The previous literature has proven that IFNs both directly and indirectly enhance the capacity of B lymphocytes to respond to viral challenge and produce cytotoxic and neutralizing antibodies [22]. We think it would be interesting to evaluate the level of HBV-specific antibodies in type I interferon receptors (IFNAR) knockout (KO) mice; however, type I interferons could inhibit hepatitis B virus replication directly [23]. Thus, the comparison of HBV-specific antibody levels between wild-type (WT) and IFNAR KO mice will be complicated.

Our findings suggest that Mn^{2+} could be used as an adjuvant in vaccination. However, more studies should be carried out to explore the potential effects of Mn^{2+} on other occasions. For example, it would be very interesting to test the effect of Mn^{2+} on the maturation of antigen-presenting cells (APCs) following T-cell activation. In the present study, we found that Mn^{2+} enhanced the HBsAg-specific antibody level after immunization of HBsAg, suggesting that Mn^{2+} may regulate antigen presentation and CD4 T-cell activation. Further studies are ongoing to characterize the effects of Mn^{2+} as an adjuvant.

CONCLUSIONS

Mn^{2+} promoted type I IFN production and could be used as an adjuvant for HBV vaccination.

Acknowledgments

Financial support. This work was supported by Quanzhou Science and Technology Project (2019N019S).

Potential conflicts of interest. The authors declare that they have no conflicts of interest. All authors have submitted the ICMJE Form for Disclosure of Potential Conflicts of Interest. Conflicts that the editors consider relevant to the content of the manuscript have been disclosed.

References

1. Glebe D. Recent advances in hepatitis B virus research: a German point of view. World J Gastroenterol **2007**; 13:8–13.
2. El-Serag HB, Rudolph KL. Hepatocellular carcinoma: epidemiology and molecular carcinogenesis. Gastroenterology **2007**; 132:2557–76.
3. Terrault NA, Bzowej NH, Chang KM, et al; American Association for the Study of Liver Diseases. AASLD guidelines for treatment of chronic hepatitis B. Hepatology **2016**; 63:261–83.

4. Conjeevaram HS, Lok AS. Management of chronic hepatitis B. J Hepatol **2003**; 38:S90–103.
5. Lee YS, Suh DJ, Lim YS, et al. Increased risk of adefovir resistance in patients with lamivudine-resistant chronic hepatitis B after 48 weeks of adefovir dipivoxil monotherapy. Hepatology **2006**; 43:1385–91.
6. De Andrea M, Ravera R, Gioia D, et al. The interferon system: an overview. Eur J Paediatr Neurol **2002**; 6:A41–6; discussion A55–8.
7. Kalvakolanu DV, Borden EC. An overview of the interferon system: signal transduction and mechanisms of action. Cancer Invest **1996**; 14:25–53.
8. Tan G, Song H, Xu F, Cheng G. When hepatitis B virus meets interferons. Front Microbiol **2018**; 9:1611.
9. Liang TJ, Block TM, McMahon BJ, et al. Present and future therapies of hepatitis B: from discovery to cure. Hepatology **2015**; 62:1893–908.
10. Wieland SF, Eustaquio A, Whitten-Bauer C, et al. Interferon prevents formation of replication-competent hepatitis B virus RNA-containing nucleocapsids. Proc Natl Acad Sci U S A **2005**; 102:9913–7.
11. Belloni L, Allweiss L, Guerrieri F, et al. IFN-α inhibits HBV transcription and replication in cell culture and in humanized mice by targeting the epigenetic regulation of the nuclear cccDNA minichromosome. J Clin Invest **2012**; 122:529–37.
12. Wang C, Guan Y, Lv M, et al. Manganese increases the sensitivity of the cGAS-STING pathway for double-stranded DNA and is required for the host defense against DNA viruses. Immunity **2018**; 48:675–687.e7.
13. Zhou W, Bi J, Janson JC, et al. Ion-exchange chromatography of hepatitis B virus surface antigen from a recombinant Chinese hamster ovary cell line. J Chromatogr A **2005**; 1095:119–25.
14. Neufeld DS. Isolation of rat liver hepatocytes. Methods Mol Biol **1997**; 75:145–51.
15. Böttinger EP, Factor VM, Tsang ML, et al. The recombinant proregion of transforming growth factor beta1 (latency-associated peptide) inhibits active transforming growth factor beta1 in transgenic mice. Proc Natl Acad Sci U S A **1996**; 93:5877–82.
16. Li PZ, Li JZ, Li M, et al. An efficient method to isolate and culture mouse Kupffer cells. Immunol Lett **2014**; 158:52–6.
17. Son EW, Lee SR, Choi HS, et al. Effects of supplementation with higher levels of manganese and magnesium on immune function. Arch Pharm Res **2007**; 30:743–9.
18. Chen P, Chakraborty S, Mukhopadhyay S, et al. Manganese homeostasis in the nervous system. J Neurochem **2015**; 134:601–10.
19. Lucifora J, Xia Y, Reisinger F, et al. Specific and nonhepatotoxic degradation of nuclear hepatitis B virus cccDNA. Science **2014**; 343:1221–8.
20. Li N, Zhang L, Chen L, et al. MxA inhibits hepatitis B virus replication by interaction with hepatitis B core antigen. Hepatology **2012**; 56:803–11.
21. Zhang R, Shu CW, Guan Y, et al. The manganese salt (MnJ) functions as a potent universal adjuvant. Biorxiv 783910 [Preprint]. 27 September **2019**. Available at: https://doi.org/10.1101/783910. Accessed 27 September 2019.
22. Kiefer K, Oropallo MA, Cancro MP, Marshak-Rothstein A. Role of type I interferons in the activation of autoreactive B cells. Immunol Cell Biol **2012**; 90:498–504.
23. Wang Y, Wei L, Jiang D, et al. In vitro resistance to interferon of hepatitis B virus with precore mutation. World J Gastroenterol **2005**; 11: 649–55.